JCTC Journal of Chemical Theory and Computation

Article

pubs.acs.org/JCTC

Applications of Time-Dependent and Time-Independent Density Functional Theory to Electronic Transitions in Tetrahedral d^0 Metal Oxides

Issaka Seidu, Mykhaylo Krykunov,* and Tom Ziegler

Department of Chemistry, University of Calgary, University Drive 2500, Calgary, AB T2N-1N4, Canada

Supporting Information

ABSTRACT: We present benchmark calculations on excitation energies based on time-dependent density functional theory (TDDFT) as well as orbital relaxed self-consistent and constricted variational DFT (RSCF-CV-DFT) with and without use of the Tamm−Dancoff approximation. The compilation contains results for the 3d complexes MnO_4^-, CrO_4^{2-}, and VO_4^{3-}, as well as the 4d congeners RuO_4, TcO_4^-, and MoO_4^{2-}, and 5d homologues OsO_4, ReO_4^-, and WO_4^{2-}. Considerations have been given to the local density approximation (LDA) and the functionals BP86 and PBE based on the generalized gradient approximation (GGA), as well as the hybrids B3LYP, BHLYP, and PBE0 and the length corrected functional LCBP86. We find for the 3d complexes that RSCF-CV-DFT fares better than TDDFT. Thus, in the case of RSCF-CV-DFT, the average root-mean-square deviations (RMSDs) are 0.25−0.3 eV for GGAs, 0.1 eV for B3LYP, and 0.45 eV for BHLYP. TDDFT affords RMSDs that on average range from 0.3 eV for local functionals to 0.7 eV for BHLYP with the largest fraction of Hartree−Fock (HF) exchange. TDDFT is seen to fare better among the heavier tetraoxo systems. For the 4d and 5d systems, the three functionals B3LYP, PBE0 with an intermediate fraction of HF exchange, and LCBP86 have the lowest RMSD of 0.2 eV, whereas the local functionals (LDA, BP86, BPE) and BHLYP with the highest HF fraction and LCBP86* have a somewhat larger RMSD of 0.3 eV. Nearly the same performance is observed for RSCF-CV-DFT with respect to the different functionals in the case of the 4d and 5d systems. Thus, for the heavier tetraoxo systems, the two DFT schemes are comparable in accuracy.

		MnO_4^-		TcO_4^-	
		B3LYP	Expt.	B3LYP	Expt.
$1t_1 \rightarrow 2e$	$1T_1$	1.65		3.98	
	$1T_2$	2.45	2.40	4.60	4.35
$2t_2 \rightarrow 2e$	$2T_1$	3.18		4.65	
	$2T_2$	3.63	3.60	5.37	5.10
$1t_1 \rightarrow 3t_2$	$1E$	3.73		5.15	
	$3T_1$	3.81		6.45	
	$3T_2$	3.85	4.10	6.38	6.60
	$1A_2$	4.21		6.78	
	RMSD	0.15		0.25	

1. INTRODUCTION

Some of the first applications of density functional theory (DFT) to chemical problems involved studies of the electronic spectrum of permanganate and related tetraoxo complexes. It was demonstrated that the Xα method[1] and kindred schemes[2−4] based on the local density approximation (LDA) could reproduce the electronic spectrum of MnO_4^- and other tetraoxo complexes with a remarkable accuracy in contrast to *ab initio* Hartree−Fock and single + double configuration interaction (SDCI) calculations.[5−8] The early DFT type calculations all employed a variational approach termed[1] ΔSCF−DFT (or simply ΔSCF) in which an excitation was represented by the promotion from the $(i)^2$ ground state configuration to the excited state configuration *ai*, and the associated excitation energy was calculated as the difference between self-consistent Kohn−Sham energies of $(i)^2$ and *ai*. The ΔSCF scheme has been applied extensively to various systems[9−11] including the tetraoxo series[2,3] with considerable success. It can be justified[12] for the first excited state with a space and spin symmetry different from that of the ground state. However, employing it to all excited states using the ground state functional has been considered *ad hoc* and unfounded in fundamental DFT theory.[13] In addition, not all transitions can be described by one Slater determinant representing a single orbital displacement $i \rightarrow a$ as it is assumed in ΔSCF. When the multi-determinantal nature of an excited state is determined by symmetry, use can be made of schemes based on the Slater sum rules[2,3] or average of configuration considerations.[14] However, the multi-determinantal nature of a state resulting from near (accidental) degeneracies of two or more electronic configurations is not well represented by ΔSCF.

In Kohn−Sham density functional theory, the natural path to excited states would seem to be the ground state response approach given the status of KS-DFT as a ground state theory. Runge and Gross[15] have given the full time-dependent extension of the ground state Kohn−Sham theory. Later, the time-dependent density functional ground state response theory (TDDFT)[16] has been formulated that in principle should be able to describe excited state properties without approximations. The exact TDDFT requires the knowledge of the "true" ground state functional as well as the frequency dependence of the energy response kernel related to this functional. In practice, one has to resort to approximate ground state functionals and neglect the frequency dependence of the

Received: March 30, 2015

DOI: 10.1021/acs.jctc.5b00298
J. Chem. Theory Comput. XXXX, XXX, XXX−XXX

kernel in what has now become known as the adiabatic TDDFT approach.[16−21] Over the past 20 years, the TDDFT approach has become the workhorse in DFT-based studies of excited states, and its strengths and weaknesses are well documented.[22−37] On the other hand, progress beyond the adiabatic approximation has been slow, although work in this direction is ongoing.[38−40] TDDFT has the distinct advantage over ΔSCF that it can deal with states that are multideterminantal. However, for the tetraoxo complexes of 3*d* metals, the simulated spectra are not in as good agreement[41,42] with experiment as ΔSCF[2,3,14] and the same can be said for many other transition metal complexes.[43] We shall from now on refer to ATDDFT as TDDFT.

We have in the last five years developed a variational approach to excited states called the constricted variational DFT method (CV-DFT)[44−52] that incorporates ΔSCF and TDDFT as special cases. In CV-DFT, we allow the occupied ground state orbitals $\{\psi_i(1);\ i = 1,...,occ\}$ to vary by mixing into each $\psi_i(1)$ a fraction of every virtual ground state orbital $\{\psi_a(1);\ a = 1,...,vir\}$ according to $\delta\psi_i \propto \sum_a U_{ai}\psi_a$. The resulting energy can be evaluated to any desired order in U_{ai}. Further, the mixing coefficients U_{ai} can be optimized variationally. It has been shown previously that the variational CV-DFT approach to second order in U_{ai} is equivalent to adiabatic TDDFT based on response theory both within the Tamm−Dancoff approximation[47] and in the general case.[51] Further, to all orders in U_{ai}, CV-DFT is equivalent to ΔSCF in those cases where the transition can be described by a single orbital replacement $\psi_i \rightarrow \psi_a$.[52]

We have in previous studies been able to treat both Rydberg[53] and charge transfer transitions[48,49] as well as other "difficult" cases such as $\pi \rightarrow \pi^*$ excitations in cyclic acenes[54] and cyanines[55] successfully even with local functionals provided that terms to all orders in U_{ai} were taken into account in our CV-DFT approach. However, this requires that U_{ai} is fully optimized[45] and that the basis of occupied $\{\psi_i(1);\ i = 1,...,occ\}$ and virtual $\{\psi_a(1);\ a = 1,...,vir\}$ ground state orbital are allowed to relax (RSCF-CV(∞)-DFT).[44,48] It is our objective in the present investigation to examine how well RSCF-CV(∞)-DFT is able to deal with the excitation energies for the series of tetraoxo complexes discussed here. We shall in our assessment compare to excitation energies from high level *ab initio* wave function methods[56−62] as well as the experiment.

2. THEORETICAL DETAILS

CV-DFT generates the KS-determinant for the one-electron transition[46]

$$\Psi' = \left|\psi_1'\psi_2'\psi_3'...\psi_i'\psi_j'...\psi_N'\right| \tag{1}$$

by making use of the unitary transformation

$$\mathbf{Y}\begin{pmatrix}\psi_{occ}\\ \psi_{vir}\end{pmatrix} = e^{\mathbf{U}}\begin{pmatrix}\psi_{occ}\\ \psi_{vir}\end{pmatrix} = \left(\sum_{m=0}^{\infty}\frac{\mathbf{U}^m}{m!}\right)\begin{pmatrix}\psi_{occ}\\ \psi_{vir}\end{pmatrix} = \begin{pmatrix}\psi'_{occ}\\ \psi'_{vir}\end{pmatrix} \tag{2}$$

among the occupied $\{\psi_k;\ k = 1,\ ...,\ occ\}$ and virtual $\{\psi_a;\ a = occ + 1,\ ...,\ occ + vir\}$ canonical orbitals of the ground state

$$\Psi^0 = \left|\psi_1\psi_2\psi_3...\psi_i\psi_j...\psi_N\right| \tag{3}$$

The transformation in CV(n)-DFT is carried out to order n in **U**.

Above, the concatenated column vectors ψ'_{occ} and ψ'_{vir} in eq 2 contain the resulting sets of occupied $\{\psi'_k;\ k = 1,...,\ occ\}$ and virtual $\{\psi'_a;\ a = occ + 1,...,\ occ + vir\}$ orbitals corresponding to an excited state due to a single electron transition. The unitary transformation matrix **Y** is in eq 2 expressed in terms of a skew symmetric matrix **U** as

$$\mathbf{Y} = e^{\mathbf{U}} = \mathbf{I} + \mathbf{U} + \frac{\mathbf{U}^2}{2} + ... = \sum_{m=0}^{\infty}\frac{\mathbf{U}^m}{m!} = \sum_{m=0}^{\infty}\frac{(\mathbf{U}^2)^m}{(2m)!} + \mathbf{U}\sum_{m=0}^{\infty}\frac{(\mathbf{U}^2)^m}{(2m+1)!} \tag{4}$$

The first occ elements in any row or column of **U** run over occupied ground state reference orbitals starting with those of α-spin. Likewise the last vir elements run over virtual ground state reference orbitals ending with those of β-spin. Further, $U_{ij} = U_{ab} = 0$ where "*i, j*" refer to the occupied set $\{\psi_i;\ i = 1,\ ...,\ occ\}$, whereas "*a, b*" refer to $\{\psi_a;\ a = occ + 1,\ ...,\ occ + vir\}$. Here, U_{ai} are the variational mixing matrix elements that combine virtual and occupied ground state orbitals in the excited state with $U_{ai} = -U_{ia}$. It is clear that the entire matrix **U** is made up of occ × vir independent elements U_{ai} that also can be organized in the column vector $\vec{U}$, where the running index now is the number of different occ/vir pairs (a, i). For a given $\vec{U}$, we can by the help of eq 4 generate a set of "occupied" excited state orbitals

$$\psi_i' = \sum_{p}^{occ+vir} Y_{pi}\psi_p = \sum_{j}^{occ} Y_{ji}\psi_j + \sum_{a}^{vir} Y_{ai}\psi_a \tag{5}$$

that are orthonormal to order n in U_{ai}.

To understand the role of different contributions into the CV(n)-DFT excitation energy, let us consider examples of different types of electronic transitions for the second and infinite order theories. In the second order scheme, the unitary transformation of eq 2 is carried out to $n = 2$, and the excited state KS orbitals are given by

$$\psi_i'(1) \rightarrow \psi(1) + \sum_{c}^{vir} U_{ci}\psi_c(1) - \frac{1}{2}\sum_{c}^{vir}\sum_{k}^{occ} U_{ci}U_{ck}\psi_k(1) + O^{(3)}[\mathrm{U}] \tag{6}$$

The corresponding energy to second order in **U** can be written as

$$\Delta E^{(2)} = \sum_{i}^{occ}\sum_{a}^{vir} U_{ai}U_{ai}[\varepsilon_a(\rho^0) - \varepsilon_i(\rho^0)] + \sum_{i}^{occ}\sum_{a}^{vir}\sum_{j}^{occ}\sum_{b}^{vir} U_{ai}U_{bj}K_{ai,bj} \tag{7}$$

which is equivalent to the energy expression of adiabatic TDDFT within the Tamm−Dancoff approximation (TDA). Here, $\varepsilon_a(\rho^0)$ and $\varepsilon_i(\rho^0)$ are the ground state orbital energies for ψ_a and ψ_i, respectively. Further,

$$K_{pq,st} = K^{\mathrm{C}}_{pq,st} + K^{\mathrm{XC}}_{pq,st} \tag{8}$$

with

$$K^{\mathrm{C}}_{pq,st} = \iint \psi_p(1)\psi_q(1)\frac{1}{r_{12}}\psi_s(2)\psi_t(2)\mathrm{d}\nu_1\mathrm{d}\nu_2 \tag{9}$$

In addition $K^{XC}_{pq,st}$ is given by

DOI: 10.1021/acs.jctc.5b00298
J. Chem. Theory Comput. XXXX, XXX, XXX−XXX

$$K_{pq,st}^{\mathrm{XC(HF)}} = -\iint \psi_p(1)\psi_s(1)\frac{1}{r_{12}}\psi_q(2)\psi_t(2)\mathrm{d}\nu_1\mathrm{d}\nu_2 \tag{10}$$

for the Hartree−Fock exchange and by

$$K_{pq,st}^{\mathrm{XC(KS)}} = \int \psi_p^{\mu}(\vec{r}_1)\psi_q^{\mu}(\vec{r}_1)f^{\mu\nu}(\vec{r}_1)\psi_s^{\nu}(\vec{r}_1)\psi_t^{\nu}(\vec{r}_1)d\vec{r} \tag{11}$$

for local KS exchange-correlation. The integration in eqs 9 and 10 is over space and spin, whereas it is over space only in eq 11. The factor $f^{\mu\nu}(\vec{r}_1)$ in eq 14 represents the normal energy kernel

$$f^{\mu\nu} = \left(\frac{\partial^2 E_{\mathrm{XC}}}{\partial\rho^{\mu}\partial\rho^{\nu}}\right)_0 \tag{12}$$

given by the functional derivative of E_{XC} with respect to the density of electrons of μ, ν spin taken at the ground state reference. If μ, ν represent opposite spin, we write the corresponding K and $K^{\mathrm{XC(KS)}}$ integrals with "bars" as $K_{pq,\bar{s}\bar{t}}$ and $K_{pq,\bar{s}\bar{t}}^{\mathrm{XC(KS)}}$, respectively. The "bars" are omitted if μ, ν comes from spin−orbitals with the same spin when we as here are dealing with systems that have a closed shell ground state.

The CV(2)-DFT/TDA excitation energy includes the configuration interaction (CI) between individual $i \rightarrow a$ and $j \rightarrow b$ transitions defined by the nondiagonal $K_{ai,bj}$ terms. This level of theory performs quite well for valence excitations in small molecules even with nonhybrid functionals.[63] The reason to go beyond the second order approximation was a necessity to describe the charge-transfer excitations.[50] Unlike adiabatic TDDFT, the infinite order theory reproduces the excitation energies for this type of transitions quite well even for local functionals.[48]

For simplicity, we shall analyze first the infinite order excitation energy for the single orbital replacement $i \rightarrow a$ transition. It is given by

$$\Delta E_{i\rightarrow a}^{(\infty)} = \varepsilon_a(\rho^0) - \varepsilon_i(\rho^0) + \frac{1}{2}K_{ii,ii} + \frac{1}{2}K_{aa,aa} - K_{ii,aa} \tag{13}$$

As it was pointed out before,[48] the $K_{ii,ii}$ and $K_{aa,aa}$ integrals combined with $\varepsilon_i(\rho^0)$ and $\varepsilon_a(\rho^0)$ represent the ionization potentials and electron affinities better than the corresponding orbital energies from standard functionals, while the $K_{ii,aa}$ integrals introduce the correct $-(1/r)$ asymptotic.[50] It should be noted here that $\varepsilon_a(\rho^0)$ is not related to the electron affinity even in exact Kohn−Sham theory.[63] The $K_{ii,ii}$ and $K_{aa,aa}$ integrals play the role of the "self-interaction" correction since they vanish in Hartree−Fock theory. Otherwise, they can be quite large. For instance, this was shown for strongly localized orbitals as in $n \rightarrow \pi^*$ transitions,[44] and apparently, it would be the case for d-orbitals in transition metals. As a result, eq 13 usually overestimates excitation energies, so an additional orbital relaxation brings a substantial correction to the total excitation energy.

The relaxation energy as well as the K integrals from eq 13 are present in a simpler theory, namely, R-CV(4)-DFT.[49] Those integrals are added in the form of the diagonal fourth order correction, but R-CV(4)-DFT was designed for transitions with $U_{ai} \approx 1$, i.e., close to the single orbital replacement type. Of course, it is necessary to include CI as in CV(2)-DFT/TDA for the general type of transitions. However, both CI and orbital relaxation might contribute to the lowering of the same excited state, which could lead to a substantial underestimation of its energy.

Let us see how this problem can be avoided. The CV(∞)-DFT[46] excitation energy expression, $\Delta E^{(\infty)}$, combines the features of eqs 7 and 13. Indeed, $\Delta E^{(\infty)}$ of the mixed state (half singlet and half triplet) is given by

$$\begin{aligned}\Delta E_M^{(\infty)} &= \sum_i^{\mathrm{occ}} \sin^2[\eta\gamma_i][\varepsilon_{i^{\mathrm{v}}}(\rho^0) - \varepsilon_{i^{\mathrm{o}}}(\rho^0)] \\ &+ \frac{1}{2}\sum_i^{\mathrm{occ}}\sum_j^{\mathrm{occ}} \sin^2[\eta\gamma_i]\sin^2[\eta\gamma_j](K_{i^{\mathrm{o}}i^{\mathrm{o}}j^{\mathrm{o}}j^{\mathrm{o}}} + K_{i^{\mathrm{v}}i^{\mathrm{v}}j^{\mathrm{v}}j^{\mathrm{v}}} - 2K_{i^{\mathrm{o}}i^{\mathrm{o}}j^{\mathrm{v}}j^{\mathrm{v}}}) \\ &+ \sum_i^{\mathrm{occ}}\sum_j^{\mathrm{occ}} \sin[\eta\gamma_i]\cos[\eta\gamma_i]\sin[\eta\gamma_j]\cos[\eta\gamma_j](K_{i^{\mathrm{o}}i^{\mathrm{v}}j^{\mathrm{o}}j^{\mathrm{v}}} + K_{i^{\mathrm{o}}i^{\mathrm{v}}j^{\mathrm{v}}j^{\mathrm{o}}})\end{aligned} \tag{14}$$

where the K integrals and orbital energies are evaluated over the natural transition orbitals (NTOs)[64,65]

$$\phi_i^{\mathrm{o}} = \sum_j^{\mathrm{occ}} W_{ji}\psi_j \tag{15}$$

$$\phi_i^{\mathrm{v}} = \sum_a^{\mathrm{vir}} V_{ai}\psi_a \tag{16}$$

They, in turn, define the excited state orbitals

$$\psi_i' = \cos[\eta\gamma_i]\phi_i^{\mathrm{o}} + \sin[\eta\gamma_i]\phi_i^{\mathrm{v}} \tag{17}$$

Further, the $\mathbf{V}$ and $\mathbf{W}$ matrices as well as γ_i values are obtained from the singular value decomposition of the transition $\mathbf{U}$ matrix. Eventually, the scaling parameter η is obtained from the normalization condition for the infinite order summation in eq 4

$$\sum_i^{\mathrm{occ}} \sin^2[\eta\gamma_i] = 1 \tag{18}$$

It can be seen that the first two terms on the r.h.s. of eq 14 contain the components of the energy expression (13), while the third term includes CI. However, all three terms in eq 14 are scaled by trigonometric functions. In order to analyze the influence of these nonlinear factors, we shall use the NTO representation because it allows us to use fewer orbitals to describe an excitation.

We shall consider first a transition from one occupied orbital to a linear combination of the virtual orbitals. This type of a transition can be obtained in the ΔSCF-DFT method. In this case, one pair of orbitals φ_k^{o}, φ_k^{v} with one singular value γ_k unequal to zero represents an excitation. The normalization condition (18), in turn, yields $\eta\gamma_k = \pi/2$ and zero for all $i \neq k$. As a result, all CI terms in eq 14 would vanish, and eq 14 will be reduced to the form of eq 13. Note that the CI terms for this type of a transition do not vanish in the second order theory. Let us now find a condition when the contribution of the CI terms is maximized.

For simplicity, we shall consider an excitation consisting of two NTO transitions with γ_i and γ_j unequal to zero. Unlike the previous one, this type of a transition cannot be a solution of the ΔSCF-DFT method. We define the two scaled singular values as $\eta\gamma_i = x$ and $\eta\gamma_j = y$, so now we need to find the maximum of the following function

$$f(x, y) = \sin(x)\cos(x)\sin(y)\cos(y) \tag{19}$$

DOI: 10.1021/acs.jctc.5b00298
J. Chem. Theory Comput. XXXX, XXX, XXX−XXX

for $0 \le x \le \pi/2$ and $0 \le y \le \pi/2$. The function $f(x, y)$ has the maximum at the point $x = \pi/4$, $y = \pi/4$, with $f(\pi/4, \pi/4) = 1/4$. Thus, in the case of excitations consisting of the linear combination of two NTO transitions with an equal contribution, the influence of CI in eq 14 is maximized. This happens when the corresponding diagonal matrix elements of the Hessian are degenerate. Such a feature of CV(∞)-DFT bears some similarity to the DFT/MRCI method of Grimme and Waletzke,[66] in which the off diagonal matrix elements are scaled with an empirical weight depending on the energy difference of two configurations. In order to preserve this effect, the orbital relaxation in the RSCF-CV(∞)-DFT scheme[44] is introduced only for the "self-interaction" terms of eq 14, which are reduced by a factor of 4 ($\sin^2(\pi/4)\sin^2(\pi/4) = 1/4$) for the last type of the considered transitions.

It should be stressed here that the orbital relaxation is evaluated only up to second order because the **R** matrix in the following unitary transformation

$$\phi_i(1) \rightarrow \psi_i(1) + \sum_c^{\mathrm{vir}} R_{ci}\psi_c(1) - \frac{1}{2}\sum_c^{\mathrm{vir}}\sum_k^{\mathrm{occ}} R_{ci}R_{ck}\psi_k(1) + O^{(3)}[R] \tag{20}$$

for the occupied

$$\phi_a(1) \rightarrow \psi_a(1) - \sum_k^{\mathrm{occ}} R_{ak}\psi_k(1) - \frac{1}{2}\sum_c^{\mathrm{vir}}\sum_k^{\mathrm{occ}} R_{ak}R_{ck}\psi_c(1) + O^{(3)}[R] \tag{21}$$

and for the virtual orbitals, respectively, is very small ($\|\mathbf{R}\| \ll 1$), and it is obtained as a response to the electronic transition defined by eq 2. Although the norm of **R** is small, the relaxation energy is not negligible, and it exceeds one eV for some of the $n \rightarrow \pi^*$ transitions.[44] Eventually, the full RSCF-CV(∞)-DFT excitation energy of the mixed state is calculated in this work according to the following formula

$$\Delta E_M^{(\infty,2)} = \Delta E_M^{(\infty)} + \Delta E_1^{\beta} + \Delta E_2^{\beta} \tag{22}$$

Here, $\Delta E_M^{(\infty)}$ is the excitation energy given by eq 14, which can be rewritten in the kernel free formulation as[46]

$$\Delta E_M^{(\infty)} = \int F_{\mathrm{KS}}^{\alpha}\left[\rho_0^{\alpha} + \frac{1}{2}\Delta\tilde{\rho}_{\alpha}^{U}, \rho_0^{\beta}\right]\Delta\tilde{\rho}_{\alpha}^{U}\,\mathrm{d}\nu + \int F_{\mathrm{KS}}^{\alpha}\left[\rho_0^{\alpha} + \frac{1}{2}\Delta\hat{\rho}_{\alpha}^{U}, \rho_0^{\beta}\right]\Delta\hat{\rho}_{\alpha}^{U}\,\mathrm{d}\nu \tag{23}$$

Here, ρ_0^{σ} is the ground state density for σ-spin, $\Delta\rho_{\alpha}^{U}$ is the density change due to an excitation. We have used the *tilde* symbol for the density change stemming from the occ-vir block of the excited state density matrix change and *hat* for the occ-occ and vir-vir blocks.[46] Two contributions to the second order relaxation energy are given by

$$\Delta E_1^{\beta} = \int F_{\mathrm{KS}}^{\beta}\left[\rho_0^{\alpha} + \Delta\hat{\rho}_{\alpha}^{U}, \rho_0^{\beta} + \frac{1}{2}\Delta\rho_{\beta}^{R(1)}\right]\Delta\rho_{\beta}^{R(1)}\mathrm{d}\nu \tag{24}$$

$$\Delta E_2^{\beta} = \int F_{\mathrm{KS}}^{\beta}[\rho_0^{\alpha} + \Delta\hat{\rho}_{\alpha}^{U}, \rho_0^{\beta}]\Delta\rho_{\beta}^{R(2)}\mathrm{d}\nu \tag{25}$$

Now, when ΔE_1^{β} and ΔE_2^{β} are also expressed in the kernel free formulation, it is easy to see that electrons in β spin−orbitals "see" a potential, which differs from the one of the ground state. This situation necessitates introducing the relaxation. The first and second order relaxation densities in eqs 24 and 25 are given by

$$\Delta\rho_{\beta}^{R(1)}(1, 1') = \sum_j^{\mathrm{occ}/2}\sum_b^{\mathrm{vir}/2} R_{bj}^{\beta}\psi_j^{\beta}(1)\psi_b^{\beta *}(1') + \sum_j^{\mathrm{occ}/2}\sum_b^{\mathrm{vir}/2} R_{bj}^{\beta}\psi_b^{\beta}(1)\psi_j^{\beta *}(1') \tag{26}$$

$$\Delta\rho_{\beta}^{R(2)}(1, 1') = \sum_{ab}^{\mathrm{vir}/2}\sum_i^{\mathrm{occ}/2} R_{ai}^{\beta}R_{bi}^{\beta}\psi_a^{\beta}(1)\psi_b^{\beta *}(1') - \sum_{ij}^{\mathrm{occ}/2}\sum_a^{\mathrm{vir}/2} R_{ai}^{\beta}R_{aj}^{\beta}\psi_i^{\beta}(1)\psi_j^{\beta *}(1') \tag{27}$$

There are two contributions to the relaxation density in eq 27 representing a change in the density. When the first term on the r.h.s. of eq 27 is integrated, it yields the charge gain, $\Delta q_{\mathrm{vir}}^{\beta} = \sum_{ai} R_{ai}^{\beta}R_{ai}^{\beta}$, in the virtual subspace, and the second one is the charge loss, $\Delta q_{\mathrm{occ}}^{\beta} = \sum_{ai} R_{ai}^{\beta}R_{ai}^{\beta}$, in the occupied subspace.

Unlike, the corresponding quantities obtained due to the transformation (2), $\Delta q_{\mathrm{occ}}^{\beta}$ and $\Delta q_{\mathrm{vir}}^{\beta}$ are not normalized to one. As a result, the total charge in the α and β manifold transferred from the occupied to the virtual subspace in RSCF-CV(∞)-DFT is not exactly one. This is similar to orthogonality constrained DFT.[67] Note that when $\mathbf{R}^{\beta}$ is normalized to one, it corresponds to promoting explicitly two electrons from the occupied to the virtual subspace: one in the α manifold and the other one in the β manifold. A procedure for the calculation of double excitations in constricted variational DFT is outlined in ref 68. In the Appendix, we have shown how not normalized $\mathbf{R}^{\beta}$ matrix connects the double with single excitations through a perturbation.

Thus, it can be seen that the inclusion of higher orders in **U** was important to make a "smooth" connection between CV(2)-DFT/TDA and R-CV(4)-DFT, while it is sufficient to have the orbital relaxation up to second order only. Nevertheless, its contribution to excitation energies in transition metal complexes is very important as it was pointed out recently.[69,70] At the same time, other authors report the failure of adiabatic TDDFT for states in transition metal complexes with strong character of double excitations.[71] So it is one of the advantages of constricted variational theory that it interconnects these two phenomena. It should be noted here that the way how double excitations are mixed to the one-electron excited states of RSCF-CV(∞)-DFT is different from the frequency/energy-dependent exchange-correlation kernels of Burke and co-workers.[38] Another distinct feature of RSCF-CV(∞)-DFT is its strong functional dependence of the singlet−triplet gap.

In CV(2)-DFT or TDDFT/TD, the triplet excitation energy for a transition involving a single orbital replacement ($i \rightarrow a$) takes on the form[55]

$$\Delta E_{\mathrm{T}}^{\mathrm{ATDDFT/TD}} = \Delta E_{\mathrm{T}}^{\mathrm{CV(2)}} = [\varepsilon_a(\rho^0) - \varepsilon_i(\rho^0)] + K_{aiai} - K_{ai\bar{a}\bar{i}} \tag{28}$$

whereas the singlet excitation energy is given by[55]

$$\Delta E_{\mathrm{S}}^{\mathrm{ATDDFT/TD}} = \Delta E_{\mathrm{S}}^{\mathrm{CV(2)}} = [\varepsilon_a(\rho^0) - \varepsilon_i(\rho^0)] + K_{aiai} + K_{ai\bar{a}\bar{i}} \tag{29}$$

DOI: 10.1021/acs.jctc.5b00298
J. Chem. Theory Comput. XXXX, XXX, XXX−XXX

Thus, the triplet-singlet separation energy in TDDFT/TD can be expressed as[55]

$$\Delta E_{S/T}^{ATDDFT/TD} = \Delta E_{S/T}^{CV(2)} = \Delta E_{S}^{CV(2)} - \Delta E_{T}^{CV(2)} = 2K_{ai\bar{a}\bar{i}} = 2K_{aiai}^{C} + 2K_{ai\bar{a}\bar{i}}^{XC} \approx \Delta \tilde{E}_{S/T}^{CV(2)} = 2K_{aiai}^{C} \quad (30)$$

Here, ≈ indicates that $2K_{ai\bar{a}\bar{i}}^{XC}$ either is zero for HF or small for KS. Thus, $\Delta \tilde{E}_{S/T}^{CV(2)}$ of eq 30 is determined by the Coulomb (but exchange type) integral $2K_{aiai}^{C}$ that has the same form for HF and KS and thus only depends indirectly on the functional through the shape of the orbitals as pointed out by Casida[16] and others.[30,55]

In RSCF-CV(∞)-DFT,[44,48] the triplet transition energy for an excitation that can be represented by a single orbital replacement ($i \rightarrow a$) takes on the form[55]

$$\Delta E_{T}^{CV(\infty)} = [\varepsilon_a(\rho^0) - \varepsilon_i(\rho^0)] + \frac{1}{2}K_{aaaa} + \frac{1}{2}K_{iiii} - K_{aa\bar{i}\bar{i}} + \Delta E_{Rel}^{T}(R) \quad (31)$$

which is also the expression for ΔSCF. Here, $\Delta E_{Rel}^{T}(R)$ is the orbital relaxation energy for RSCF-CV(∞)-DFT. This energy is zero for the CV(2) method. The corresponding singlet energy is given by[55]

$$\Delta E_{S}^{CV(\infty)} = [\varepsilon_a(\rho^0) - \varepsilon_i(\rho^0)] + \frac{1}{2}K_{aaaa} + \frac{1}{2}K_{iiii} - 2K_{aaii} + K_{aa\bar{i}\bar{i}} + \Delta E_{Rel}^{S}(R) \quad (32)$$

whereas the singlet−triplet separation takes on the form[55]

$$\Delta E_{S/T}^{CV(\infty)} = \Delta E_{S}^{CV(\infty)} - \Delta E_{T}^{CV(\infty)} = -2K_{aaii} + 2K_{aa\bar{i}\bar{i}} + \Delta E_{Rel}^{S}(R) - \Delta E_{Rel}^{T}(R) \approx -2K_{aaii}^{XC} \quad (33)$$

where ≈ again means that we in a qualitative discussion of our quantitative calculations with all terms included will neglect $\Delta E_{Rel}^{S}(R) - \Delta E_{Rel}^{T}(R)$ and $2K_{rr\bar{v}\bar{v}}^{XC}$. For functionals with a fraction $\alpha(0.0 \le \alpha \le 1.0)$ of HF exchange, we get

$$\Delta \tilde{E}_{S/T}^{CV(\infty)} = -2K_{aaii}^{XC(Hyb)} = -2(1-\alpha)K_{aaii}^{XC(KS)} - 2\alpha K_{aaii}^{XC(HF)} = -2(1-\alpha)K_{aaii}^{XC(KS)} + 2\alpha K_{aiai}^{C} \quad (34)$$

Thus, since from observations

$$0.0 < -K_{aaii}^{XC(KS)} < K_{aiai}^{C} \quad (35)$$

we find in general $\Delta \tilde{E}_{S/T}^{CV(\infty)} < \Delta \tilde{E}_{S/T}^{CV(2)}$ for pure DFT. However, as the fraction α of HF exchange increases, the difference decreases until pure HF with $\alpha = 1$, where $\Delta \tilde{E}_{S/T}^{CV(\infty)} = \Delta \tilde{E}_{S/T}^{CV(2)}$. Thus, the expression for $\Delta \tilde{E}_{S/T}^{CV(\infty)}$ is strongly functional dependent in contrast to $\Delta \tilde{E}_{S/T}^{CV(2)}$.[30,55] We shall in the following simply refer to RSCF-CV(∞)-DFT as RSCF-CV-DFT.

3. COMPUTATIONAL DETAILS

We have carried out all DFT calculations by employing a developers version of the ADF 2012 program.[72] Our calculations employed a standard triple-ζ Slater type orbital (STO) basis with one (TZP)[73] or two (TZ2P)[73] sets of polarization functions for all atoms. Use was made of the local density approximation in the VWN parametrization[74] and the BP86 generalized gradient approximation (GGA) with the correlation part by Perdew[75] and the exchange part by Becke.[76] We employed further the B3LYP and BHLYP hybrid functional by Becke[77] with the correlation functional taken from Lee et al.[78] Here, B3LYP has 20% Hartree−Fock exchange, whereas BHLYP has 50%. Employed as well was the PBE[79] and PBE0[80,81] functionals, where the latter has 25% HF exchange.

We have finally applied the length corrected functionals (LC). In the LC-functional, the regions of electron−electron interaction are divided into "long" and "short" range parts by dividing the Coulomb operator into two pieces:

$$1/r_{12} = SR + LR = \frac{w(\omega, r_{12})}{r_{12}} + \frac{1 - w(\omega, r_{12})}{r_{12}} \quad (36)$$

where r_{12} is the interelectronic distance $r_{12} = |\vec{r}_1 - \vec{r}_2|$, whereas w is some kind of continuous switching function that goes to 1 as r_{12} goes to zero and to zero as r_{12} becomes large. The parameter ω determines how rapidly the switching occurs. This type of division has been introduced by a number of groups to combine DFT and wave function theory.[32,33] The most widely used form for $w(\omega,r_{12})$ is the error function[32,33] as it gives rise to integrals that are readily evaluated in connection with Gaussian basis sets. An alternative choice is the exponential function

$$w(\omega, r_{12}) = \exp(-\omega r_{12}) \quad (37)$$

which in combination with the r_{12}^{-1} operator gives the Yukawa potential.[82−84] The exponential choice for $w(\omega,r_{12})$ in eq 37 has been used for both Gaussian[82,83] and Slater type basis sets.[84] We employ here $w(\omega,r_{12})$ in eq 37 with $\omega = 0.40$ and $\omega = 0.75$ when nothing else is mentioned. The local functional employed in conjunction with LC was BP86. Here, LC combined with BP86 for $\omega = 0.40$ is termed LCBP86 whereas the combination with $\omega = 0.75$ is called LCBP86*.

All electrons were treated variationally without resorting to the frozen core approximation.[72] The parameter for the precision of the numerical integration was set to a (standard) value of 5.0. A special auxiliary STO basis was employed to fit the electron density in each cycle for an accurate representation of the exchange and Coulomb potentials.[72] Experimental structures idealized to tetrahedral T_d symmetry were used throughout.[14]

4. RESULTS AND DISCUSSION

We compile in the Supporting Information (SI) calculated excitation energies based on TDDFT as well as RSCF-CV-DFT with and without the use of the Tamm−Dancoff approximation.[85] The compilation contains results for the 3d complexes MnO_4^-, CrO_4^{2-}, and VO_4^{3-}, as well as their 4d congeners RuO_4, TcO_4^-, and MoO_4^{2-}, and 5d homologues OsO_4, ReO_4^-, and WO_4^{2-}. Considerations have been given to LDA and the GGAs BP86 and PBE, as well as the hybrids B3LYP, BHLYP, and PBE0 and the length corrected functionals LCBP86 and LCBP86* (see Computational Details).

The valence excitations in tetraoxo complexes involve the removal of an electron from the $1t_1$, $2t_2$, 1a, 1e, and $1t_2$ levels represented by pure ligand orbitals ($1t_1$) or ligand dominated orbitals ($2t_2$, 1a, 1e, and $1t_2$) with an in-phase metal d-based orbitals component. The electron goes to a d-orbital with out-of-phase ligand contributions (2e, $3t_2$) (Figures 1 and 2). The

DOI: 10.1021/acs.jctc.5b00298
J. Chem. Theory Comput. XXXX, XXX, XXX−XXX

electronic spectrum of the prototypical tetraoxo system permanganate (MnO_4^-) has been studied extensively by both experimental and computational techniques.

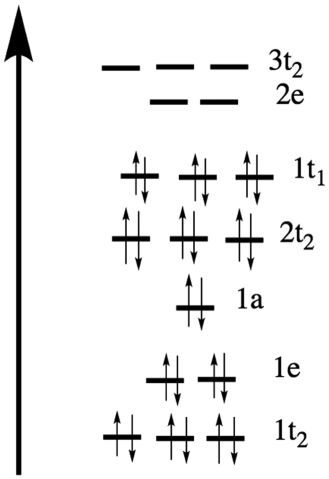

Figure 1. Orbital level diagram for d^0 tetraoxo complexes.

The first *ab initio* studies were on the Hartree−Fock level[5,6,56] followed by configuration interaction with both singles and doubles (CISD),[7,8] symmetry adapted cluster-configuration interaction (SAC-CI),[57] equation of motion coupled cluster (EOM-CCSD) schemes,[58−61] and self-consistent restricted active space (RASSCF or simply RAS) methods with a second order perturbation theory (PT2) correction,[60] as well as second (CC2) and third order (CC3) coupled cluster response theory.[61] We compare in Table 1 the calculated excitation energies for the first three dipole allowed transitions to singlet T_2 states with the experiment. For the variational methods (HF, CISD, SAC-CI, RAS-PT2), we note a clear convergence toward the experimental values in going from the simplest (HF) to the most extensive *ab initio* scheme (RAS-PT2). On the other hand, the two response methods CC2 and CC3 are seen to fail, whereas CR-EOM-CCSD(T)[60] affords results quite similar to RAS-PT2.[60] The excellent performance of RAS-PT2 testifies to the fact that static correlation is important for the description of MnO_4^-.[4,62]

The excited states of permanganate have also been studied by DFT schemes based on either variation or response theory. All the variational studies have so far adopted the ΔSCF approach.[1] In the earlier ΔSCF applications, use was made of only the exchange part of the LDA functional (X_α)[3,86] often in connection with the scattered wave approximation (SW-X_α).[87] Later on, both exchange and correlation from the LDA functional have been included in the ΔSCF calculations.[14] The agreement with the experiment[88,89] is good as shown in Table 2. A more resent approach is the density functional theory-based multi-reference configuration interaction (DFT/MRCI) scheme by Grimme and Waletzke.[66] It is similar to regular MRCI except that the diagonal terms are based on DFT. The off-diagonal terms are evaluated as in MRCI but scaled by a function that contains five global parameters obtained from a fit so as to reproduce a small set of experimental data. The calculated excitation energies[90] are quite good given that MnO_4^- was not in the training set (Table 2).

Published response-based DFT studies of permanganate are limited to adiabatic TDDFT calculations.[41,60,91−94] They include[41,93,94] two investigations in which the full vibronic fine structure is simulated. The excitation energies afforded by TDDFT for MnO_4^- are in general too high when experimental structures are used (Table 2). We shall return to this point later.

For both ΔSCF and TDDFT, there are several computational parameters that influence the calculated excitation energies aside from the use of a specific functional. One is the size of the basis set used. For the three lowest valence excitations involving transitions from $1t_1$, $2t_2$ to 2e, $3t_2$, we find a TZ2P basis to be adequate (converged), in line with previous observations.[92] The excitation energies from the corresponding smaller basis TZP differ typically by 0.05 eV from the TZ2P results and tend to be lower (SI). Another factor is geometry. Usually optimized structures have somewhat longer M−O distances than experimental geometries.[14,60,92] We shall here make use of experimental structures in order to keep the number of computational variables at a minimum. Our choice

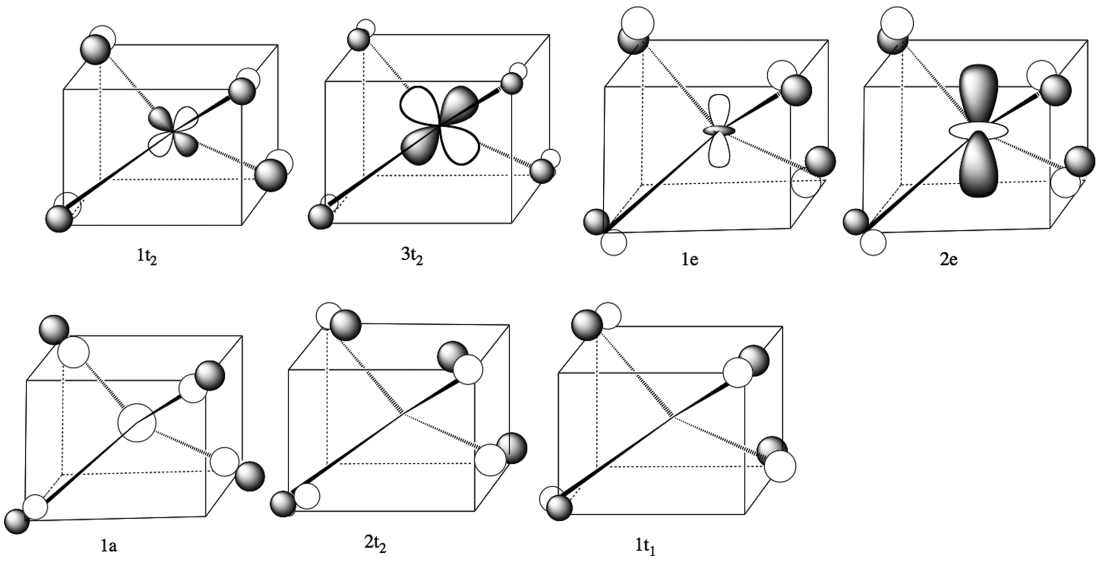

Figure 2. Frontier molecular orbitals of d^0 tetraoxo complexes.

DOI: 10.1021/acs.jctc.5b00298
J. Chem. Theory Comput. XXXX, XXX, XXX−XXX

Table 1. Calculated Excitation Energies[a,b] for MnO_4^- Based on *ab initio* Wave Function Methods

	HF[56]	SDCI[7]	SAC-CI[57]	EOM[60]	RAS-PT2[60]	CC2[61]	CC3[61]	exp.[88]
	1.04	2.60	2.57	2.50	2.33	0.18	−0.34	2.40
	2.54	4.10	3.58	3.83	3.53	1.86	1.39	3.60
	2.94	4.50	3.72	4.03	4.20			4.10
RMSD	1.20	0.39	0.24	0.15	0.08	2.00	2.49	
MAE	1.19	0.37	0.19	0.13	0.08	1.99	2.48	

[a]Energies in eV. [b]First three dipole allowed transitions to singlet T_2 states.

Table 2. Calculated Excitation Energies[a,b] for MnO_4^- based on DFT Methods

SW-Xα[87]	Xα[3,86]	ΔSCF-LDA[14]	TDDFT-SAOP[91c]	TDDFT-B3LYP[60]	DFT/MRCI[90]	exp.[88]
2.30	2.48	2.71	3.08	2.81	2.74	2.40
3.30	3.96	4.02	4.12	3.88	4.21	3.60
4.70	4.15	4.22	5.01	4.41	4.80	4.10

[a]Energies in eV. [b]First three dipole-allowed transitions to singlet T_2 states. [c]Long length corrected functional.

Table 3. RMSDs for Tetraoxo Excitation Energies Based on TDDFT and a TZ2P Basis Set[a,b,c,d,e]

compound	LDA	BP86	PBE	B3LYP	BHLYP	PBE0	LCBP86	LCBP86*
MnO_4^-	0.50	0.51	0.52	0.44	0.39	0.48	0.42	0.34
CrO_4^{2-}	0.23	0.24	0.31	0.39	0.75	0.54	0.50	0.64
VO_4^{3-}	0.10	0.12	0.13	0.44	1.04	0.59	0.47	0.87
RuO_4	0.38	0.39	0.39	0.32	0.22	0.34	0.33	0.26
TcO_4^-	0.13	0.12	0.26	0.22	0.43	0.29	0.27	0.55
MoO_4^{2-}	0.21	0.20	0.20	0.12	0.64	0.23	0.22	0.63
OsO_4	0.34	0.37	0.38	0.34	0.32	0.38	0.37	0.39
ReO_4^-	0.33	0.31	0.30	0.16	0.26	0.14	0.12	0.28
WO_4^{2-}	0.56	0.52	0.51	0.19	0.36	0.09	0.08	0.40
average 3d[f]	0.28	0.29	0.32	0.42	0.73	0.54	0.46	0.62
average 4d+5d[g]	0.32	0.31	0.34	0.24	0.36	0.26	0.25	0.41
total average[h]	0.30	0.30	0.33	0.31	0.49	0.37	0.33	0.49

[a]Root mean square deviation. [b]Reference is the observed vertical excitation energies for the three first dipole allowed transitions. [c]For MoO_4^{2-} and WO_4^{2-} only, the first two experimental transitions are available. [d]Deviations are in eV. [e]No Tamm−Dancoff approximation was applied. [f]Average of the three 3d complexes [g]Average of the six 4d and 5d complexes. [h]Average over all complexes.

Table 4. RMSDs for Tetroxo Excitation Energies Based on RSCV-CV(∞)-DFT and a TZ2P Basis Set[a,b,c,d,e]

compound	LDA	BP86	PBE	B3LYP	BHLYP	PBE0	LCBP86	LCBP86*
MnO_4^-	0.41	0.32	0.33	0.15	0.62	0.19	0.24	0.37
CrO_4^{2-}	0.40	0.31	0.34	0.09	0.55	0.04	0.22	0.32
VO_4^{3-}	0.25	0.14	0.16	0.07	0.18	0.14	0.27	0.37
RuO_4	0.32	0.28	0.28	0.21	0.44	0.22	0.19	0.31
TcO_4^-	0.10	0.13	0.13	0.25	0.13	0.29	0.27	0.17
MoO_4^{2-}	0.14	0.23	0.23	0.06	0.22	0.18	0.13	0.34
OsO_4	0.53	0.51	0.50	0.27	0.39	0.31	0.21	0.26
ReO_4^-	0.36	0.43	0.43	0.14	0.25	0.16	0.14	0.16
WO_4^{2-}	0.43	0.51	0.51	0.14	0.11	0.07	0.11	0.16
average 3d[f]	0.35	0.26	0.28	0.10	0.45	0.12	0.24	0.35
average 4d+5d[g]	0.31	0.34	0.34	0.19	0.27	0.22	0.19	0.24
total average[h]	0.33	0.31	0.32	0.16	0.34	0.18	0.21	0.28

[a]Root mean square deviation. [b]Reference is the observed vertical excitation energies for the three first dipole allowed transitions. [c]For MoO_4^{2-} and WO_4^{2-} only, the first two experimental transitions are available. [d]Deviations are in eV. [e]No Tamm−Dancoff approximation was applied. [f]Average of the three 3d complexes. [g]Average of the six 4d and 5d complexes. [h]Average over all complexes.

typically leads to higher excitation energies (0.1−0.3 eV) than those obtained from optimized geometries.

Many of the tetraoxo systems are anions with spectra observed in solution or a host crystal. We find solvation in the form of COSMO[95,96] to have a marginal influence on the calculated excitation energies (0.01−0.02 eV) for the transitions considered here as already noted by others (SI).[60,94] This is also confirmed by a recent ingenious experiment[89] where the permanganate spectrum was recorded in vacuum and found to be blue-shifted by only 0.15 eV compared to solution. This is in contrast to the higher transitions from the ligands to diffuse metal s and p orbitals where solvation must be included in a proper description.[92] Since these higher transitions are not considered in this work, the comparisons are made with experimental results in solution only. For both TDDFT and RSCF-CV-DFT, we have finally the choice of conducting

DOI: 10.1021/acs.jctc.5b00298
J. Chem. Theory Comput. XXXX, XXX, XXX−XXX

Table 5. Calculated Excitation Energies Based on RSCV-CV(∞)-DFT and TDDFT for MnO_4^- and TcO_4^-[a,b]

method	LDA	BP86	PBE	B3LYP	BHLYP	PBE0	LCBP86	LCBP86*	Exp.
MnO_4^-									
TDDFT	2.86	2.87	2.87	2.88	2.98	2.92	2.81	2.82	2.40[88]
	3.93	3.93	3.94	3.96	3.93	4.02	3.99	3.96	3.60
	4.76	4.77	4.78	4.57	4.23	4.58	4.55	4.29	4.10
RSCF-CV-DFT	2.67	2.65	2.65	2.45	2.12	2.52	2.68	2.62	2.40
	3.96	3.86	3.86	3.63	2.64	3.71	3.85	3.99	3.60
	4.66	4.52	4.54	3.85	3.72	3.83	3.93	4.16	4.10
TcO_4^-									
TDDFT	4.48	4.48	4.47	4.57	4.74	4.62	4.61	4.82	4.35[98]
	5.19	5.20	5.20	5.40	5.71	5.49	5.48	5.87	5.10
	6.45	6.47	6.17	6.65	6.76	6.74	6.68	6.89	6.60
RSCF-CV-DFT	4.51	4.50	4.49	4.60	4.33	4.63	4.57	4.46	4.35
	5.01	4.93	4.93	5.37	5.15	5.49	5.43	5.27	5.10
	6.61	6.59	6.53	6.38	6.38	6.46	6.36	6.38	6.60

[a]TZ2P basis without use of the Tamm-Dancoff approximation. [b]Energies in eV.

Table 6. [a,b]Comparisons between Multiplet Splittings Calculated by Different Methods for MnO_4^- and TcO_4^-

	MnO_4^-									
	TDDFT	RAS-PT2[61]	SAC-CI[61]	RSCF-CV-DFT	exp.[88]	TDDFT	RAS-PT2[61]	SAC-CI[61]	RSCF-CV-DFT	exp.[98]
singlet										
$1T_1$	2.35	1.93	2.18	1.65		4.17	3.84	3.83	3.98	
$1T_2$	2.88	2.33	2.57	2.45	2.40	4.57	4.19	4.28	4.60	4.35
$2T_1$	3.74	3.39	3.33	3.18		4.80	4.66	4.61	4.65	
$2T_2$	3.96	3.53	3.58	3.63	3.60	5.40	5.08	5.29	5.37	5.10
1E	4.10	3.90	3.41	3.73		5.41	5.29	4.98	5.15	
$3T_1$	4.22	3.93	4.12	3.81		6.22	5.53	6.42	6.45	
$3T_2$	4.57	4.20	3.72	3.85	4.10	6.65	6.07	6.20	6.38	6.60
$1A_2$	4.16	3.89	4.46	4.21		6.43	6.04	6.54	6.78	
RMSD	0.44	0.05	0.24	0.15		0.32	0.26	0.25		

[a]TZ2P basis without use of the Tamm−Dancoff approximation used for TDDFT and RSCF-CV-DFT. [b]Energies in eV.

calculations with or without the Tamm−Dancoff approximation (TDA).[85] Our calculations reveal that the use of the TDA approximations has a minor influence on the calculated excitation energies with estimates that are typically slightly higher (0.05 to 0.1 eV) than those from a full calculation (SI).

Table 3 displays root-mean-square deviations (RMSD) between the first three experimental dipole allowed transitions and the corresponding values calculated by TDDFT with a TZ2P basis. In total, nine complexes were considered. In Table 4, the same data for the RSCF-CV-DFT method are given. Table 5 provides actual calculated excitation energies based on TDDFT and RSCF-CV-DFT in comparison with experiment for MnO_4^- and TcO_4^-. Here, the former is a representative for the 3d complexes, whereas the latter typifies the heavier congeners.

For MnO_4^-, the TDDFT energies are uniformly too high compared to experiment. This is a general trend for the 3d complexes where the TDDFT RMSDs on average range from 0.3 eV for local functionals to 0.7 eV for BHLYP with the largest fraction of HF exchange. In the case of RSCF-CV-DFT, the MnO_4^- energies are somewhat too high (0.2 eV) for the local functionals and too low for BHLYP (0.3 eV), whereas B3LYP affords the best agreement with the experiment. These RSCF-CV-DFT trends are typical for all the 3d complexes where the average RMSDs are 0.25−0.3 eV for GGAs, 0.1 eV for B3LYP, and 0.45 eV for BHLYP.

TDDFT is seen to fare better among the heavier tetraoxo systems than the 3d homologous as exemplified by TcO_4^-. On average, the three functionals B3LYP, PBE0 with an intermediate fraction of HF exchange, and LCBP86 have the lowest RMSD of 0.2 eV, whereas the local functionals (LDA, BP86, BPE) and BHLYP with the highest HF fraction and LCBP86* have a somewhat larger RMSD of 0.3 eV. Interestingly enough, the heavier tetraoxo systems reveal the same trend among the different functionals for RSCF-CV-DFT with a RMSD of 0.2 eV for B3LYP, PBE0, and LCBP86 and 0.3 eV for the remaining functionals. Thus, for the heavier tetraoxo complexes, RSCF-CV-DFT does not constitute a clear improvement over TDDFT, which already is quite good. However, for the 3d complexes where the calculated TDDFT energies are too high, the RSCF-CV-DFT scheme seems to fare better at least for B3LYP.

The RSCF-CV-DFT scheme is in principle able to resolve not only the T_2 excited state energy terms but all multiplets. We compare in Table 6 multiplet energies based on RSCF-CV-DFT and TDDFT with those obtained from the high-level wave function methods[60] RAS-PT2 and SAC-CI for MnO_4^- and TcO_4^-. Here, the DFT calculations made use of B3LYP. The first excitation in MnO_4^- and TcO_4 is dominated by the $t_1 \rightarrow 2e$ orbital transition, which gives rise to the $1T_1$ and $1T_2$ multiplets. All methods find the order $1T_1 < 1T_2$, which is in agreement with the experiment.[97] A rough experimental estimate[98] of 0.5 eV is also in reasonable agreement with the

DOI: 10.1021/acs.jctc.5b00298
J. Chem. Theory Comput. XXXX, XXX, XXX−XXX

Table 7. [a,b]Calculated Triplet−Singlet Separation Energies for the First Three T_2 States in MnO_4^- and TcO_4^- Based on RSCF-CV(∞)-DFT and TDDFT

method	State	LDA	BP86	PBE	B3LYP	BHLYP	PBE0
TDDFT (MnO_4^-)							
	$1T_2$	0.94	0.94	0.94	1.40	2.08	1.56
	$2T_2$	0.55	0.56	0.56	0.85	1.24	0.93
	$3T_2$	0.82	0.80	0.80	0.91	1.20	0.90
RSCF-CV-DFT (MnO_4^-)							
	$1T_2$	0.61	0.75	0.73	1.21	1.81	1.36
	$2T_2$	0.46	0.53	0.51	0.82	0.96	0.92
	$3T_2$	0.60	0.51	0.51	0.60	0.55	0.62
TDDFT (TcO_4^-)							
	$1T_2$	0.89	0.88	0.87	1.16	1.72	1.24
	$2T_2$	0.82	0.85	0.84	1.09	1.47	1.17
	$3T_2$	0.71	0.69	0.67	0.62	0.54	0.60
RSCF-CV-DFT (TcO_4^-)							
	$1T_2$	0.61	0.74	0.72	1.17	1.34	1.10
	$2T_2$	0.48	0.55	0.53	0.84	1.28	0.92
	$3T_2$	0.46	0.44	0.43	0.58	0.66	0.53

[a]TZ2P basis without use of the Tamm−Dancoff approximation. [b]Energies in eV.

calculated splittings. Here, RSCF-CV-DFT affords the largest estimate of 0.8 eV. The sizes of the DFT splittings are strongly functional dependent and tend to increase with the fraction of HF exchange. The second excitation has a large contribution from the $2t_2 \rightarrow 2e$ orbital transition. It gives rise to the $2T_1$ and $2T_2$ terms that again unanimously are calculated to have the order $2T_1 < 2T_2$. There is no experimental information available. The third excitation is in part due to the $1t_1 \rightarrow 3t_2$ orbital transition with the multiplets 1E, $3T_1$, $3T_2$, and $1A_2$. Here, 1E is in all cases of lowest energy, whereas $1A_2$ is at (or near) the top. For $3T_1$ and $3T_2$, the order $3T_1 < 3T_2$ is observed for all methods in the MnO_4^- case as well as TDDFT and RAS-PT2 in TcO_4^-, whereas it is reversed for SIC-CI and RSCF-CV-DFT for the same molecule, and this is also the order obtained for CR-EOM-CCSD(T).[60] Again, experimental data is not available. It is obvious that more work on better-characterized systems has to be carried out to assess the ability of RSCF-CV-DFT to resolve multiplets.

To date, the triplet T_2 spin multiplets have eluded observation in spite of many attempts to characterize these presumably very short-lived states.[99] For TDDFT and RSCF-CV-DFT, the triplet−singlet splittings are in most cases calculated to be somewhat larger for the more compact 3d complexes such as permanganate than the larger congeners such as TcO_4^- (Table 7).

It follows from eqs 28−30 that the TDDFT/TD splitting for a $i \rightarrow a$ transition is given by $\Delta\tilde{E}_{S/T}^{CV(2)} = 2K_{aiai}^{C}$, where K_{aiai}^{C} is a Coulomb integral defined in eq 9. This expression is only indirectly functional dependent through the shape of the orbitals *a,i*. However, we clearly see this dependence in Table 7, where $\Delta\tilde{E}_{S/T}^{CV(2)} = 2K_{aiai}^{C}$ increases with the fraction (α) of HF exchange. The dependence reflects the decline in covalency with a growing α, which leads to both M−O bonding ($i = 2t_2$, 1a, 1e, and $1t_2$) and antibonding ($a = 2e$, $3t_2$) orbitals being increasingly polarized toward M or O.[4] Similar trends are seen for calculations without the TD approximation.

The triplet−singlet separation in RSCF-CV-DFT/TD is according to eq 34 given by $\Delta\tilde{E}_{S/T}^{CV(\infty)} = -2(1-\alpha)K_{aaii}^{XC(KS)} + 2\alpha K_{aiai}^{C}$ for a $i \rightarrow a$ transition. Here, α is again the HF fraction, K_{aiai}^{C} is the Coulomb integral discussed above, and $K_{aaii}^{XC(KS)} = K_{aiai}^{XC(KS)}$ is the local exchange correlation term defined in eq 11. Since from experience $0.0 < -K_{aaii}^{XC(KS)} < K_{aiai}^{C}$, we find that $\Delta\tilde{E}_{S/T}^{CV(2)} > \Delta\tilde{E}_{S/T}^{CV(\infty)}$ for the local functionals with $\alpha = 0$ (Table 7). The fact that $\Delta\tilde{E}_{S/T}^{CV(2)} > \Delta\tilde{E}_{S/T}^{CV(\infty)}$ is in part responsible for the observation that TDDFT affords higher excitation energies that are higher than RSCF-CV-DFT. As we add HF exchange and increase α, $\Delta\tilde{E}_{S/T}^{CV(\infty)}$ should approach $\Delta\tilde{E}_{S/T}^{CV(2)}$. However, it follows from Table 7 that the two have not yet converged for BHLYP with $\alpha = 0.50$.

5. CONCLUDING COMMENTS

We have for the first time probed the ability of our newly developed RSCF-CV-DFT scheme to describe excited states of transition metal complexes. Use was made of the tetrahedral d^0 metal oxides as the first benchmark series since the tetra oxides have a long history as a challenging testing ground for new methods due to their complex electronic structure. We have investigated nine systems with three members from each transition series using eight different functionals and compared the results to findings based on TDDFT and experiment. We find for the 3d systems MnO_4^-, CrO_4^{2-}, and VO_4^{3-} that RSCF-CV-DFT affords excitation energies in better agreement with the experiment than TDDFT for each of the functionals discussed here. The best agreement (RMSD 0.1 eV) was obtained with the B3LYP and PBEO hybrid functionals holding relatively modest HF exchange contributions of 20% and 25%, respectively. Local functionals fared slightly worse, whereas a substantial increase in HF exchange as in BHLYP leads to sizable deviations (RMSD = 0.45 eV). By comparison the TDDFT method tends to provide excitation energies for the 3d complexes that are uniformly too high (Table 3 and SI). For the heavier 4d and 5d congeners, we find that RSCF-CV-DFT and TDDFT performs equally well with the smallest RMSDs of 0.2 eV encountered for B3LYP and PBEO.

Work is now under way to benchmark RSCF-CV-DFT for other transition metal systems where accurate observations and high-level calculations are available. The benchmarking will also involve other properties such as the first order change in density with respect to *U* that represents the transition density as well as the higher order change that express the "active" charge rearrangement. Here direct comparison can be made to TDDFT that also provides both types of density change.

DOI: 10.1021/acs.jctc.5b00298
J. Chem. Theory Comput. XXXX, XXX, XXX−XXX

However, in contrast to TDDFT, but in common with ΔSCF, our RSCF-CV-DFT scheme also affords orbital relaxation in response to the "active" density change. Thus, in a transition represented by the orbital replacement $t_1 \rightarrow 2e$, the "active" change in density would be given by $\Delta\rho_{\text{active}} = 2e2e - 1t_1 1t_1$, which represents a charge transfer from the ligands to the d-orbitals making the metal center more electron rich. However, as shown previously in connection with ΔSCF, relaxation of the other orbitals tends to reduce or completely reduce the charge build-up on the metal. Thus, we hope that RSCF-CV-DFT will provide more realistic information about the total charge rearrangement involved in an excitation than TDDFT.

APPENDIX

We shall now consider the procedure for the calculation of the $\mathbf{R}^{\beta}$ matrix in RSCF-CV(∞)-DFT. First, the gradient of eq 22 with respect to $\mathbf{R}^{\beta}$ is given by

$$\frac{\mathrm{d}\Delta E_M^{(\infty,2)}}{\mathrm{d}R_{ai}^{\beta}} = \int F_{\mathrm{KS}}^{\beta}[\rho_0^{\alpha} + \Delta\hat{\rho}_{\alpha}^{U}, \rho_0^{\beta} + \Delta\rho_{\beta}^{R(1)}]\left[\frac{\partial\Delta\rho_{\beta}^{R(1)}}{\partial R_{ai}^{\beta}}\right]_0 \mathrm{d}\nu + \int F_{\mathrm{KS}}^{\beta}[\rho_0^{\alpha} + \Delta\hat{\rho}_{\alpha}^{U}, \rho_0^{\beta}]\left[\frac{\partial\Delta\rho_{\beta}^{R(2)}}{\partial R_{ai}^{\beta}}\right]_0 \mathrm{d}\nu = V_{ai} \tag{A1}$$

where

$$\frac{\partial\Delta\rho_{\beta}^{R(1)}}{\partial R_{ai}^{\beta}} = \psi_a^{\beta *}(1)\psi_i^{\beta}(1') + \psi_i^{\beta *}(1)\psi_a^{\beta}(1') \tag{A2}$$

$$\frac{\partial\Delta\rho_{\beta}^{R(2)}}{\partial R_{ck}^{\beta}} = 2\sum_{a}^{\mathrm{vir}/2} R_{ak}^{\beta}\psi_a^{\beta}(1)\psi_c^{\beta *}(1') - 2\sum_{j}^{\mathrm{occ}/2} R_{cj}^{\beta}\psi_k^{\beta}(1)\psi_j^{\beta *}(1') \tag{A3}$$

Here, "*i, j, k*" refer to the occupied canonical orbitals and "*a, b, c*" to the virtual ones. Note that the derivatives in eq A1 are taken at $\mathbf{R}^{\beta} = \mathbf{R}_0^{\beta}$, which means that the second term in eq A1 is zero at the very first iteration. Thus, the gradient is reduced in that case to

$$V_{ai}^{(0)} = \int F_{\mathrm{KS}}^{\beta}[\rho_0^{\alpha} + \Delta\hat{\rho}_{\alpha}^{U}, \rho_0^{\beta}][\psi_a^{\beta *}(1)\psi_i^{\beta}(1') + \psi_i^{\beta *}(1)\psi_a^{\beta}(1')]\mathrm{d}\nu \tag{A4}$$

Now by making use of the Tailor series expansion for the Fock operator

$$\int F_{\mathrm{KS}}[\rho_0 + \Delta\rho_1]\Delta\rho_2 \mathrm{d}\nu = \int F_{\mathrm{KS}}[\rho_0]\Delta\rho_2 \mathrm{d}\nu + \iint \Delta\rho_1 f_{\mathrm{HXC}}\Delta\rho_2 \mathrm{d}\nu_1 \mathrm{d}\nu_2 \tag{A5}$$

eq A4 can be rewritten as

$$V_{ai}^{(0)} = \sum_{bc}\sum_{ai}\Delta\hat{P}_{bc}^{U}K_{bc,\bar{a}\bar{i}} + \sum_{jk}\sum_{ai}\Delta\hat{P}_{jk}^{U}K_{jk,\bar{a}\bar{i}} \tag{A6}$$

Here, $\Delta\hat{P}^{U}$ is the density matrix corresponding to the transition defined by eq 2,[46] and the K integrals are defined by eqs 8−11.

However, the same type of integrals as in eq A6 is evaluated in wave function theory as the matrix elements between the following Slater determinants[100]

$$|...\psi_c^{\alpha}\psi_i^{\beta}...| \xrightarrow{K_{bc,\bar{a}\bar{i}}} |...\psi_b^{\alpha}\psi_a^{\beta}...| \tag{A7}$$

$$|...\psi_k^{\alpha}\psi_i^{\beta}...| \xrightarrow{K_{jk,\bar{a}\bar{i}}} |...\psi_j^{\alpha}\psi_a^{\beta}...| \tag{A8}$$

i.e., they describe the interaction between the single and double electron transitions.

Further, the Hessian of eq 22 with respect to $\mathbf{R}^{\beta}$ is given by

$$\frac{\mathrm{d}^2\Delta E_M^{(\infty,2)}}{\mathrm{d}R_{ai}^{\beta}\mathrm{d}R_{bj}^{\beta}} = K_{\bar{a}\bar{i},\bar{b}\bar{j}} + K_{\bar{a}\bar{i},\bar{j}\bar{b}} + \int F_{\mathrm{KS}}^{\beta}[\rho_0^{\alpha} + \Delta\hat{\rho}_{\alpha}^{U}, \rho_0^{\beta}]\left[\frac{\partial^2\Delta\rho_{\beta}^{R(2)}}{\partial R_{ai}^{\beta}\partial R_{bj}^{\beta}}\right]_0 \mathrm{d}\nu = H_{\bar{a}\bar{i},\bar{b}\bar{j}} \tag{A9}$$

$$\frac{\partial^2\Delta\rho_{\beta}^{R(2)}}{\partial R_{ai}^{\beta}\partial R_{bj}^{\beta}} = \psi_a^{\beta}(1)\psi_b^{\beta *}(1')\delta_{\bar{i}\bar{j}} - \psi_i^{\beta}(1)\psi_j^{\beta *}(1')\delta_{\bar{a}\bar{b}} \tag{A10}$$

Here, we have used "bars" over indices in order to indicate β spin−orbitals. It can be seen that the Hessian defined by eqs A9 and A10 differs from the one of the second order theory. Namely, the orbital energies are calculated not at the ground state density but at the density corresponding to the infinite order excitation energy. On the basis of eqs A1 and A9, the $\mathbf{R}^{\beta}$ matrix is obtained from the following response equation

$$\mathbf{R}^{\beta} = \mathbf{H}^{-1}\mathbf{V} \tag{A11}$$

which is solved iteratively in RSCF-CV(∞)-DFT.

Alternatively, the inverse of $\mathbf{H}$ can be obtained from its spectral resolution

$$\mathbf{R}^{\beta} = \sum_{I}\frac{1}{\omega_I}(\mathbf{U}^{I\beta} \otimes \mathbf{U}^{I\beta})\mathbf{V} \tag{A12}$$

where ⊗ is the Kronecker or outer product, and ω_I and $\mathbf{U}^{I\beta}$ are the Ith eigenvalue of $\mathbf{H}$ and its eigenvector:

$$\mathbf{H}\mathbf{U}^{I\beta} = \omega_I\mathbf{U}^{I\beta} \tag{A13}$$

The summation in eq A12 is over all one-electron excitations of the singly excited state Hessian $\mathbf{H}$. Equation A12 can also be rewritten for each matrix element as

$$R_{ai}^{\beta} = \sum_{I} U_{ai}^{I\beta}C^{I\beta} \tag{A14}$$

where

$$C^{I\beta} = \frac{1}{\omega_I}\sum_{bj} U_{bj}^{I\beta}V_{bj} \tag{A15}$$

Thus, $C^{I\beta}$ values play the role of CI coefficients for the doubly excited states, when $\mathbf{R}^{\beta}$ from eq A14 is substituted into the RSCF-CV(∞)-DFT KS-determinant:

DOI: 10.1021/acs.jctc.5b00298
J. Chem. Theory Comput. XXXX, XXX, XXX−XXX

$$\Psi_M^{U,R} = |\psi_1'^{\alpha}...\psi_i'^{\alpha}...\psi_N'^{\alpha}\phi_1^{\beta}...\phi_i^{\beta}...\phi_N^{\beta}| \rightarrow |\psi_1'^{\alpha}...\psi_i'^{\alpha}...\psi_N'^{\alpha}\psi_1^{\beta}...\psi_i^{\beta}...\psi_N^{\beta}| + \sum_I C^{I\beta}|\psi_1'^{\alpha}...\psi_i'^{\alpha}...\psi_N'^{\alpha}\phi_1^{I\beta}...\phi_i^{I\beta}...\phi_N^{I\beta}| + O^{(2)}[\mathbf{R}] \quad \text{(A16)}$$

with

$$\phi_i^{I\beta} = \sum_a^{\text{vir}/2} U_{ai}^{I\beta}\psi_a^{\beta} \quad \text{(A17)}$$

It should be stressed here that although eq A16 formally includes the summation over all eigenvectors of **H**, only a few of them are actually included due to the perturbation operator **V** and inverse eigenvalues.

■ ASSOCIATED CONTENT

Supporting Information

Excitation energies calculated with the RSCF-CV-DFT and TDDFT methods. The Supporting Information is available free of charge on the ACS Publications website at DOI: 10.1021/acs.jctc.5b00298.

■ AUTHOR INFORMATION

Corresponding Author

*E-mail: mkrykuno@ucalgary.ca.

Notes

The authors declare no competing financial interest.
Tom Ziegler passed away in March 2015.

■ ACKNOWLEDGMENTS

The authors thank NSERC for financial support.

■ REFERENCES

(1) Slater, J. C. Statistical Exchange-Correlation in the Self-Consistent Field. *Adv. Quantum Chem.* **1972**, *6*, 1−92.
(2) Ziegler, T.; Rauk, A.; Baerends, E. J. The electronic structures of tetrahedral oxo-complexes. The nature of the "charge transfer" transitions. *Chem. Phys.* **1976**, *16*, 209−217.
(3) Ziegler, T.; Rauk, A.; Baerends, E. J. On the calculation of multiplet energies by the hartree-fock-slater method. *Theor. Chim. Acta* **1977**, *43*, 261−271.
(4) Buijse, M.; Baerends, E. J. Analysis of nondynamical correlation in the metal−ligand bond. Pauli repulsion and orbital localization in MnO_4^-. *J. Chem. Phys.* **1990**, *93*, 4129−4141.
(5) Hillier, H.; Saunders, V. R. Ab initio Molecular Orbital Calculations of the Ground and Excited States of the Permanganate and Chromate Ions. *Proc. R. Soc. London, Ser. A* **1970**, *320*, 161−173.
(6) Hillier, H.; Saunders, V. R. Ab initio calculations of the excited states of the permanganate and chromate ions. *Chem. Phys. Lett.* **1971**, *9*, 219−221.
(7) Johansen, H.; Rettrup, S. Limited configuration interaction calculation of the optical spectrum for the permanganate ion. *Chem. Phys.* **1983**, *74*, 77−81.
(8) Johansen, H. Analysis of a configuration interaction calculation for a charge transfer transition in MnO_4^-. *Mol. Phys.* **1983**, *49*, 1209−1216.
(9) Besley, N.; Gilbert, A.; Gill, P. Self-consistent-field calculations of core excited states. *J. Chem. Phys.* **2009**, *130*, 124308.
(10) Gavnholt, J.; Olsen, T.; Engelund, M.; Schiøtz, J. Δself-consistent field method to obtain potential energy surfaces of excited molecules on surfaces. *Phys. Rev. B: Condens. Matter Mater. Phys.* **2008**, *78*, 075441.
(11) Kowalczyk, T.; Yost, S. R.; Van Voorhis, T. Assessment of the ΔSCF density functional theory approach for electronic excitations in organic dyes. *J. Chem. Phys.* **2011**, *134*, 054128.
(12) Gunnarsson, O.; Lundqvist, B. I. Exchange and correlation in atoms, molecules, and solids by the spin-density-functional formalism. *Phys. Rev. B* **1976**, *13*, 4274−4298.
(13) von Barth, U. Local-density theory of multiplet structure. *Phys. Rev. A: At., Mol., Opt. Phys.* **1979**, *20*, 1693−1703.
(14) Stückl, A. C.; Daul, C. A.; Güdel, H. Excited-state energies and distortions of d^0 transition metal tetraoxo complexes: A density functional study. *J. Chem. Phys.* **1997**, *107*, 4606−4617.
(15) Runge, E.; Gross, E. K. U. Density-Functional Theory for Time-Dependent Systems. *Phys. Rev. Lett.* **1984**, *52*, 997−1000.
(16) Casida, M. E. Time-Dependent Density Functional Response Theory for Molecules. In *Recent Advances in Density Functional Methods*; Chong, D. P., Ed.; World Scientific: Singapore, 1995; Vol. *1*, pp 155−193.
(17) van Gisbergen, S. J. A.; Snijders, J. G.; Baerends, E. J. A density functional theory study of frequency-dependent polarizabilities and Van der Waals dispersion coefficients for polyatomic molecules. *J. Chem. Phys.* **1995**, *103*, 9347−9354.
(18) Petersilka, M.; Gossmann, U. J.; Gross, E. K. U. Excitation Energies from Time-Dependent Density-Functional Theory. *Phys. Rev. Lett.* **1996**, *76*, 1212−1215.
(19) Bauernschmitt, R.; Ahlrichs, R. Treatment of electronic excitations within the adiabatic approximation of time dependent density functional theory. *Chem. Phys. Lett.* **1996**, *256*, 454−464.
(20) Furche, F. On the density matrix based approach to time-dependent density functional response theory. *J. Chem. Phys.* **2001**, *114*, 5982−5992.
(21) Furche, F.; Ahlrichs, R. J. Adiabatic time-dependent density functional methods for excited state properties. *J. Chem. Phys.* **2002**, *117*, 7433−7447.
(22) Romaniello, P.; Sangalli, D.; Berger, J. A.; Sottile, F.; Molinari, L. G.; Reining, L.; Onida, G. Double excitations in finite systems. *J. Chem. Phys.* **2009**, *130*, 044108.
(23) Gritsenko, O.; Baerends, E. J. Double excitation effect in non-adiabatic time-dependent density functional theory with an analytic construction of the exchange−correlation kernel in the common energy denominator approximation. *Phys. Chem. Chem. Phys.* **2009**, *11*, 4640−4646.
(24) Jacquemin, D.; Wathelet, V.; Perpète, E. A.; Adamo, C. Extensive TD-DFT Benchmark: Singlet-Excited States of Organic Molecules. *J. Chem. Theory Comput.* **2009**, *5*, 2420−2435.
(25) Jacquemin, D.; Perpète, E. A.; Ciofini, I.; Adamo, C. Accurate Simulation of Optical Properties in Dyes. *Acc. Chem. Res.* **2009**, *42*, 326−334.
(26) Jacquemin, D.; Perpete, E. A.; Scuseria, G. E.; Ciofini, I.; Adamo, C. TD-DFT Performance for the Visible Absorption Spectra of Organic Dyes: Conventional versus Long-Range Hybrids. *J. Chem. Theory Comput.* **2008**, *4*, 123−135.
(27) Grimme, S.; Neese, F. Double-hybrid density functional theory for excited electronic states of molecules. *J. Chem. Phys.* **2007**, *127*, 154116.
(28) Send, R.; Valsson, O.; Filippi, C. Electronic Excitations of Simple Cyanine Dyes: Reconciling Density Functional and Wave Function Methods. *J. Chem. Theory Comput.* **2011**, *7*, 444−455.
(29) Jacquemin, D.; Zhao, Y.; Valero, R.; Adamo, C.; Ciofini, I.; Truhlar, D. G. Verdict: Time-Dependent Density Functional Theory "Not Guilty" of Large Errors for Cyanines. *J. Chem. Theory Comput.* **2012**, *8*, 1255−1259.
(30) Moore, B., II; Autschbach, J. Longest-Wavelength Electronic Excitations of Linear Cyanines: The Role of Electron Delocalization and of Approximations in Time-Dependent Density Functional Theory. *J. Chem. Theory Comput.* **2013**, *9*, 4991−5003.
(31) Schipper, P. R. T.; Gritsenko, O. V.; van Gisbergern, S. J. A.; Baerends, E. J. Molecular calculations of excitation energies and (hyper)polarizabilities with a statistical average of orbital model exchange-correlation potentials. *J. Chem. Phys.* **2000**, *112*, 1344−1352.

DOI: 10.1021/acs.jctc.5b00298
J. Chem. Theory Comput. XXXX, XXX, XXX−XXX

(32) Iikura, H.; Tsuneda, T.; Yanai, T.; Hirao, K. A long-range correction scheme for generalized-gradient-approximation exchange functionals. *J. Chem. Phys.* **2001**, *115*, 3540−3544.
(33) Song, J.-W.; Watson, M. A.; Hirao, K. An improved long-range corrected hybrid functional with vanishing Hartree−Fock exchange at zero interelectronic distance (LC2gau-BOP). *J. Chem. Phys.* **2009**, *131*, 144108.
(34) Heyd, J.; Scuseria, G. E.; Ernzerhof, M. Hybrid functionals based on a screened Coulomb potential. *J. Chem. Phys.* **2003**, *118*, 8207−8215.
(35) Baer, R.; Neuhauser, D. Density Functional Theory with Correct Long-Range Asymptotic Behavior. *Phys. Rev. Lett.* **2005**, *94*, 043002.
(36) Dreuw, A.; Weisman, J.; Head-Gordon, M. Long-range charge-transfer excited states in time-dependent density functional theory require non-local exchange. *J. Chem. Phys.* **2003**, *119*, 2943−2946.
(37) Tozer, D. Relationship between long-range charge-transfer excitation energy error and integer discontinuity in Kohn−Sham theory. *J. Chem. Phys.* **2003**, *119*, 12697−12699.
(38) Cave, R. J.; Zhang, F.; Maitra, N. T.; Burke, K. A dressed TDDFT treatment of the 2^1A_g states of butadiene and hexatriene. *Chem. Phys. Lett.* **2004**, *389*, 39−42.
(39) Mazur, G.; Wlodarczyk, R. Application of the dressed time-dependent density functional theory for the excited states of linear polyenes. *J. Comput. Chem.* **2009**, *30*, 811−817.
(40) Elliott, P.; Goldson, S.; Canahui, C.; Maitra, N. T. Perspectives on double-excitations in TDDFT. *Chem. Phys.* **2011**, *391*, 110−119.
(41) Jose, L.; Seth, M.; Ziegler, T. Molecular and Vibrational Structure of Tetroxo d^0 Metal Complexes in their Excited States. A Study Based on Time-Dependent Density Functional Calculations and Franck−Condon Theory. *J. Phys. Chem. A* **2012**, *116*, 1864−1876.
(42) Neugebauer, J.; Baerends, E. J.; Nooijen, M. Vibronic Structure of the Permanganate Absorption Spectrum from Time-Dependent Density Functional Calculations. *J. Phys. Chem. A* **2005**, *109*, 1168−1179.
(43) Rudolph, M.; Ziegler, T.; Autschbach, J. Time-dependent density functional theory applied to ligand-field excitations and their circular dichroism in some transition metal complexes. *Chem. Phys.* **2011**, *391*, 92−100.
(44) Krykunov, M.; Ziegler, T. Self-consistent Formulation of Constricted Variational Density Functional Theory with Orbital Relaxation. Implementation and Applications. *J. Chem. Theory Comput.* **2013**, *9*, 2761−2773.
(45) Ziegler, T.; Krykunov, M.; Cullen, J. The implementation of a self-consistent constricted variational density functional theory for the description of excited states. *J. Chem. Phys.* **2012**, *136*, 124107.
(46) Cullen, J.; Krykunov, M.; Ziegler, T. The formulation of a self-consistent constricted variational density functional theory for the description of excited states. *Chem. Phys.* **2011**, *391*, 11−18.
(47) Ziegler, T.; Seth, M.; Krykunov, M.; Autschbach, J.; Wang, F. On the relation between time-dependent and variational density functional theory approaches for the determination of excitation energies and transition moments. *J. Chem. Phys.* **2009**, *130*, 154102.
(48) Krykunov, M.; Seth, M.; Ziegler, T. Introducing constricted variational density functional theory in its relaxed self-consistent formulation (RSCF-CV-DFT) as an alternative to adiabatic time dependent density functional theory for studies of charge transfer transition. *J. Chem. Phys.* **2014**, *140*, 18A502.
(49) Ziegler, T.; Krykunov, M. On the calculation of charge transfer transitions with standard density functionals using constrained variational density functional theory. *J. Chem. Phys.* **2010**, *133*, 074104.
(50) Ziegler, T.; Seth, M.; Krykunov, M.; Autschbach, J. A revised electronic Hessian for approximate time-dependent density functional theory. *J. Chem. Phys.* **2008**, *129*, 184114.
(51) Ziegler, T.; Krykunov, M.; Autschbach, J. Derivation of the RPA (Random Phase Approximation) Equation of ATDDFT (Adiabatic Time Dependent Density Functional Ground State Response Theory) from an Excited State Variational Approach Based on the Ground State Functional. *J. Chem. Theory Comput.* **2014**, *10*, 3980−3986.
(52) Park, Y. C.; Krykunov, M.; Ziegler, T. On the relation between adiabatic time dependent density functional theory (TDDFT) and the ΔSCF-DFT method. Introducing a numerically stable ΔSCF-DFT scheme for local functionals based on constricted variational DFT. *Mol. Phys.* **2015**, *113*, 1636−1647.
(53) Seidu, I.; Krykunov, M.; Ziegler, T. Applications of Time-Dependent and Time-Independent Density Functional Theory to Rydberg Transitions. *J. Phys. Chem. A* **2015**, *119*, 5107−5116.
(54) Krykunov, M.; Grimme, S.; Ziegler, T. Accurate Theoretical Description of the ^1L_a and ^1L_b Excited States in Acenes Using the All Order Constricted Variational Density Functional Theory Method and the Local Density Approximation. *J. Chem. Theory Comput.* **2012**, *8*, 4434−4440.
(55) Zhekova, H.; Krykunov, M.; Autschbach, J.; Ziegler, T. Applications of Time Dependent and Time Independent Density Functional Theory to the First π to π^* Transition in Cyanine Dyes. *J. Chem. Theory Comput.* **2014**, *10*, 3299−3307.
(56) Hsu, H.; Peterson, C.; Pitzer, R. M. Calculations on the permanganate ion in the ground and excited states. *J. Chem. Phys.* **1976**, *64*, 791−795.
(57) Nakai, H.; Ohmori, Y.; Nakatsuji, H. Theoretical study on the ground and excited states of MnO^-_4. *J. Chem. Phys.* **1991**, *95*, 8287−8291.
(58) Nooijen, M. Combining coupled cluster and perturbation theory. *J. Chem. Phys.* **1999**, *111*, 10815−10826.
(59) Nooijen, M.; Lotrich, V. Extended similarity transformed equation-of-motion coupled cluster theory (extended-STEOM-CC): Applications to doubly excited states and transition metal compounds. *J. Chem. Phys.* **2000**, *113*, 494−507.
(60) Su, J.; Xu, W.-H.; Xu, C.-F.; Schwarz, W. H. E.; Li, J. Theoretical Studies on the Photoelectron and Absorption Spectra of MnO_4^- and TcO_4^-. *Inorg. Chem.* **2013**, *52*, 9867−9874.
(61) Almeida, N. M. S.; McKinlay, R. G.; Paterson, M. J. Excited Electronic States of MnO_4^-: Challenges for Wavefunction and Density Functional Response Theories. *Chem. Phys.* **2015**, *446*, 86−91.
(62) Ziegler, T. A Chronicle About the Development of Electronic Structure Theories for Transition Metal Complexes. *Struct. Bonding (Berlin)* **2011**, *47*, 1−38.
(63) Baerends, E. J.; Gritsenko, O. V.; van Meer, R. The Kohn-Sham gap, the fundamental gap and the optical gap: the physical meaning of occupied and virtual Kohn-Sham orbital energies. *Phys. Chem. Chem. Phys.* **2013**, *15*, 16408−16425.
(64) Martin, R. L. Natural transition orbitals. *J. Chem. Phys.* **2003**, *118*, 4775−4777.
(65) Amos, A. T.; Hall, G. G. Single determinant wave functions. *Proc. R. Soc. London, Ser. A* **1961**, *263*, 483−493.
(66) Grimme, S.; Waletzke, M. A combination of Kohn−Sham density functional theory and multi-reference configuration interaction methods. *J. Chem. Phys.* **1999**, *111*, 5645−5655.
(67) Evangelista, F. A.; Shushkov, P.; Tully, J. C. Orthogonality constrained density functional theory for electronic excited states. *J. Phys. Chem. A* **2013**, *117*, 7378−7392.
(68) Seidu, I.; Krykunov, M.; Ziegler, T. The formulation of a constricted variational density functional theory for double excitations. *Mol. Phys.* **2014**, *112*, 661−668.
(69) Peng, B.; van Kuiken, B. E.; Ding, X.; Li, X. Guided Self-Consistent-Field Method for Excited-State Wave Function Optimization: Applications to Ligand-Field Transitions in Transition-Metal Complexes. *J. Chem. Theory Comput.* **2013**, *9*, 3933−3938.
(70) Zhekova, H.; Seth, M.; Ziegler, T. A Perspective on the Relative Merits of Time-Dependent and Time-Independent Density Functional Theory in Studies of the Electron Spectra Due to Transition Metal Complexes. An Illustration Through Applications to Copper Tetrachloride and Plastocyanin. *Int. J. Quantum Chem.* **2014**, *114*, 1019−1029.
(71) Vlahović, F.; Perić, M.; Gruden-Pavlović, M.; Zlatar, M. Assessment of TD-DFT and LF-DFT for study of $d - d$ transitions in first row transition metal hexaaqua complexes. *J. Chem. Phys.* **2015**, *142*, 214111.

DOI: 10.1021/acs.jctc.5b00298
J. Chem. Theory Comput. XXXX, XXX, XXX−XXX

(72) te Velde, G.; Bickelhaupt, F. M.; van Gisbergen, S. J. A.; Fonseca Guerra, C.; Baerends, E. J.; Snijders, J. G.; Ziegler, T. Chemistry with ADF. *J. Comput. Chem.* **2001**, *22*, 931−967.
(73) Van Lenthe, E.; Baerends, E. J. Optimized Slater-type basis sets for the elements 1−118. *J. Comput. Chem.* **2003**, *24*, 1142−1156.
(74) Vosko, S. H.; Wilk, L.; Nusair, M. Accurate spin-dependent electron liquid correlation energies for local spin density calculations: a critical analysis. *Can. J. Phys.* **1980**, *58*, 1200−1211.
(75) Perdew, J. P. Density-functional approximation for the correlation energy of the inhomogeneous electron gas. *Phys. Rev. B: Condens. Matter Mater. Phys.* **1986**, *33*, 8822−8824.
(76) Becke, A. D. Density-functional exchange-energy approximation with correct asymptotic behavior. *Phys. Rev. A: At., Mol., Opt. Phys.* **1988**, *38*, 3098−3100.
(77) Becke, A. D. A new mixing of Hartree−Fock and local density-functional theories. *J. Chem. Phys.* **1993**, *98*, 1372−1377.
(78) Lee, C.; Yang, W.; Parr, R. G. Development of the Colle-Salvetti correlation-energy formula into a functional of the electron density. *Phys. Rev. B: Condens. Matter Mater. Phys.* **1988**, *37*, 785−789.
(79) Perdew, J. P.; Burke, K.; Ernzerhof, M. Perdew, Burke, and Ernzerhof Reply. *Phys. Rev. Lett.* **1998**, *80*, 891.
(80) Ernzerhof, M.; Scuseria, G. Assessment of the Perdew−Burke−Ernzerhof exchange-correlation functional. *J. Chem. Phys.* **1999**, *110*, 5029−5036.
(81) Adamo, C.; Barone, V. Toward reliable density functional methods without adjustable parameters: The PBE0 model. *J. Chem. Phys.* **1999**, *110*, 6158−6170.
(82) Akinaga, Y.; Ten-no, S. Range-separation by the Yukawa potential in long-range corrected density functional theory with Gaussian-type basis functions. *Chem. Phys. Lett.* **2008**, *462*, 348−351.
(83) Akinaga, Y.; Ten-no, S. Intramolecular charge-transfer excitation energies from range-separated hybrid functionals using the Yukawa potential. *Int. J. Quantum Chem.* **2009**, *109*, 1905−1914.
(84) Seth, M.; Ziegler, T. Range-Separated Exchange Functionals with Slater-Type Functions. *J. Chem. Theory Comput.* **2012**, *8*, 901−907.
(85) Hirata, S.; Head-Gordon, M. Time-dependent density functional theory within the Tamm−Dancoff approximation. *Chem. Phys. Lett.* **1999**, *314*, 291−299.
(86) Ziegler, T.; Rauk, A.; Baerends, E. J. The electronic structures of tetrahedral oxo-complexes. The nature of the "charge transfer" transitions. *Chem. Phys.* **1976**, *16*, 209−217.
(87) Johnson, K. H.; Smith, F. C., Jr. Scattered-wave model for the electronic structure and optical properties of the permanganate ion. *Chem. Phys. Lett.* **1971**, *10*, 219−223.
(88) Holt, S. L.; Ballhausen, C. J. Low temperature absorption spectra of $KMnO_4$ in $KClO_4$. *Theor. Chim. Acta* **1967**, *7*, 313−320.
(89) Houmøller, J.; Kaufman, S. H.; Støchkel, K.; Tribedi, L. C.; Brøndsted Nielsen, S.; Weber, J. M. On the Photoabsorption by Permanganate Ions in Vacuo and the Role of a Single Water Molecule. New Experimental Benchmarks for Electronic Structure Theory. *ChemPhysChem* **2013**, *14*, 1133−1137.
(90) Escudero, D.; Thiel, W. Assessing the density functional theory-based multireference configuration interaction (DFT/MRCI) method for transition metal complexes. *J. Chem. Phys.* **2014**, *140*, 194105.
(91) van Gisbergen, S. J. A.; Snijders, J. G.; Baerends, E. J. Implementation of time-dependent density functional response equations. *Comput. Phys. Commun.* **1999**, *118*, 119−138.
(92) Boulet, P.; Chermette, H.; Daul, C.; Gilardoni, F.; Rogemond, F.; Weber, J.; Zuber, G. Absorption Spectra of Several Metal Complexes Revisited by the Time-Dependent Density-Functional Theory-Response Theory Formalism. *J. Phys. Chem. A* **2001**, *105*, 885−894.
(93) Dierksen, M.; Grimme, S. Density functional calculations of the vibronic structure of electronic absorption spectra. *J. Chem. Phys.* **2004**, *120*, 3544−3554.
(94) Dierksen, M.; Grimme, S. The Vibronic Structure of Electronic Absorption Spectra of Large Molecules: A Time-Dependent Density Functional Study on the Influence of "Exact" Hartree−Fock Exchange. *J. Phys. Chem. A* **2004**, *108*, 10225−10237.
(95) Klamt, A.; Schüürmann, G. COSMO: A new approach to dielectric screening in solvent with explicit expressions for the screening energy and its gradient. *J. Chem. Soc., Perkin Trans. 2* **1993**, *2*, 799−805.
(96) Pye, C. C.; Ziegler, T. An implementation of the conductor-like screening model of solvation within the Amsterdam density functional package. *Theor. Chem. Acc.* **1999**, *101*, 396−408.
(97) Ballhausen, C. J.; Trabjerg, I. Confirmation of the red band system in MnO_4^- as $^1T_1 \leftarrow {}^1A_1$ from the effect of pressure on single crystal absorption spectra. *Mol. Phys.* **1972**, *24*, 689−693.
(98) Güdel, H. U.; Ballhausen, C. J. Low temperature absorption spectra of TcO_4^- and ReO_4^- in $KClO_4$. *Theor. Chim. Acta* **1972**, *25*, 331−337.
(99) Coremans, C. J. M; van der Waals, J. H.; Konijnenberg, J.; Huizer, A. H.; Varma, C. A. G. O. A search for the metastable triplet states of CrO_4^{2-} and MnO_4^- by transient absorption spectroscopy in crystals at low temperature. *Chem. Phys. Lett.* **1986**, *125*, 514−519.
(100) Szabo, A.; Ostlund, N. S. Many-Electron Wave Functions and Operators. In *Modern Quantum Chemistry*; Dover Publications, Inc: Mineola, NY, 1996; pp 70−72.

DOI: 10.1021/acs.jctc.5b00298
J. Chem. Theory Comput. XXXX, XXX, XXX−XXX